High-bandwidth millimetre wave multiple-input multiple-output antenna for 38 GHz 5G mobile applications

Md. Ashraful Haque[1], Md. Kawsar Ahmed[1], Narinderjit Singh Sawaran Singh[2], Md. Afzalur Rahman[3], Md. Sharif Ahammed[1], Redwan A. Ananta[1], Kamal Hossain Nahin[1], Jamal Hossain Nirob[1], Liton Chandra Paul[4]

[1]Department of Electrical and Electronic Engineering, Daffodil International University, Dhaka, Bangladesh
[2]Faculty of Data Science and Information Technology, INTI International University, Nilai, Malaysia
[3]Space Science Centre, Climate Change Institute, Universiti Kebangsaan Malaysia (UKM), Bangi, Malaysia
[4]Department of Electrical, Electronic and Communication Engineering, Pabna University of Science and Technology, Pabna, Bangladesh

Article Info

ABSTRACT

This study assesses the efficacy of an industrial and innovation antenna by scrutinizing its performance using simulations and an equivalent resistor, inductor, and capacitor (RLC) circuit model. By utilizing computer simulation technology (CST) modeling techniques, the antenna's small dimensions of 37.75×31.75 mm^2 are considered concerning the minimum frequency. The antenna functions at a frequency of 38 GHz, with a bandwidth of 11 GHz. It has a maximum gain of 8.875 dB and demonstrates excellent isolation (-27.627 dB) and efficiency (98.859%), respectively. By designing and simulating a comparable RLC circuit in advanced design system (ADS), we have confirmed the accuracy and reliability of the data acquired via CST. Both CST and ADS simulators yielded similar reflection coefficients. This antenna is a superb option for the 38 GHz frequency range in 5G wireless communication.

Corresponding Author:

Narinderjit Singh Sawaran Singh
Faculty of Data Science and Information Technology, INTI International University
Persiaran Perdana BBN, Putra Nilai, Nilai 71800, Negeri Sembilan, Malaysia
Email: narinderjits.sawaran@newinti.edu.my

1. INTRODUCTION

The millimetre wave (mm-Wave) frequency spectrum, the band in which a 5G antenna operating at 38 GHz operates, is essential for providing the low latency and high data throughput that 5G networks claim to offer. However, although they have a reduced range and may require a line-of-sight connection due to the higher frequency, these antennas offer low latency and high transmission rates [1]. These antennas' total performance and coverage are improved thanks to their compact design and ability to support multiple-input multiple-output (MIMO) functionality. Applications such as augmented and virtual reality (AR/VR), autonomous vehicles (AVs), and real-time gaming depend on the antenna's ability to provide low-latency transmission [2]. High-bandwidth antennas for mobile applications are necessary to support modern wireless communications, such as 4th generation long-term evolution (4G LTE) and 5th generation (5G) networks [3]. These antennas may provide scientists with enhanced connectivity, reduced latency, and increased data transmission speeds, among other potential benefits [4]. The following is a list of properties and variants of high-band antennas compatible with mobile devices. The omnidirectional signal propagation these antennas provide allows them to cover a significant amount of ground. They are compatible with handheld devices and operate effectively in urban and suburban environments [5]. The technology known as MIMO, which stands

for multiple inputs and multiple outputs, is a crucial element of 5G wireless communication systems. Through the enhancement of data throughput, the improvement of signal quality, and the enhancement of the overall network capacity, the performance of 5G networks is improved [6]. The design and implementation of MIMO systems can be complex, and it is necessary to consider the placement and orientation of these antennas. Optimizing the gain and performance of 5G antennas can be accomplished by applying machine learning (ML) techniques. The complex and ever-changing nature of wireless networks can be better managed with the help of these strategies, which can also improve the system's overall performance. When attempting to predict antenna gain with a regression model, it is necessary to use previous data on antenna features and network circumstances to train a machine-learning model. Given new data to be input, the trained model can then make predictions regarding the gain of an antenna.

This research examines and contrasts many characteristics, including resonance frequency, size, bandwidth, gain, isolation component carrier leakage (CCL), and efficiency. Despite its compact size, the suggested antenna exhibits exceptional isolation and gain and offers the widest bandwidth. The computer simulation technology (CST) simulations demonstrate a gain of 8.875 dB, which exceeds the gains reported in the literature of 7.9 dB, 4.85 dB, 1.83 dB, 8.1 dB, 8.2 dB, and 5.3 dB [7]-[12]. Based on CST analysis, the suggested design has a bandwidth of around 11 GHz, higher than the bandwidths claimed by several sources, ranging from 1.2 GHz to 6 GHz. The proposed design demonstrates isolation values beyond 27 dB, in contrast to the isolation values of 28 dB, 24 dB, 20 dB, and 22 dB reported in the reference works [7]-[9], [12]. The proposed MIMO antenna performs well, with an error correction code (ECC) of less than 0.0003 and a diversity gain (DG) above 9.99 dB. The efficiency of the proposed MIMO antenna is 98.859%, while the reference works [8], [10], [12] have efficiencies of 85%, 76%, and 90%, respectively. The sources do not utilize the resistor, inductor, and capacitor (RLC) equivalent circuit findings essential to the providing architecture. The suggested design broadly services ML, a concept that needs a more precise definition in the relevant literature.

2.   DESIGN METHOD

In this section, we will explore the geometrical construction of the single-element 38 GHz antenna that has been proposed for use. We will identify the most suitable design parameters to consider while designing this antenna. This will give us a detailed perception of the antenna's physical structure and how it has been optimized to perform at its best.

2.1. Single element

The antenna is made specifically to work at a frequency of 38 GHz. Figure 1 shows the detailed construction of our proposed single-element antenna. Figure 1(a) illustrates the front side, showcasing the key design features and structural components. Meanwhile, Figure 1(b) presents the back side, highlighting the ground plane and other relevant elements. Single-element antenna design is the thought of making and compacting antenna sizes [13]. We pick a dielectric component identified as Rogers RT 5880 (lossy), with dimensions of $7 \times 7 \times 1.57$ mm^3. The specifications of our suggested antenna are as follows: the patch length (Lp) is 4 mm, the patch width (Wp) is 3.88889 mm, and the thickness (t) is 0.035 mm. The patch and ground are constructed of the same copper metal (annealed). Ls=7 mm, Ws=7 mm, st=1.57 mm, bl=7 mm, bw=7 mm, r=1 mm, d=2.70 mm, s11=8 mm, Sw1=5 mm, fw=0.7 mm, and fl=3.6 mm.
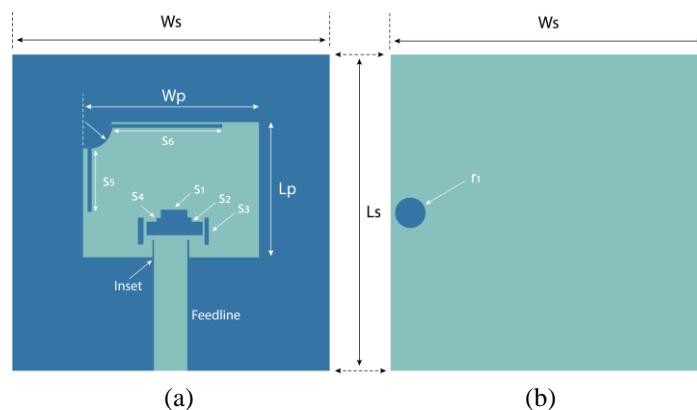

Figure 1. Proposed single element antenna of view; (a) front and (b) back

2.2. Array antenna

While achieving our final or proposed antenna, the second step was to design the array antenna. Figure 2 provides an illustration of the proposed array antenna. Figure 2(a) displays the front side, while Figure 2(b) shows the back side of the array antenna. One of the most important parts was measuring the length and width of the feed line to ensure better antenna performance, which had an impedance of 50 ohms [14]. We also calculated the impedance for feedline 2, shown in Figure 2, to be 70 ohms, while the impedance for feedline three was set to 100 ohms. For measurements, we used 1.70×2.84 mm^2 length and width for feedline one and 0.90×7.25 mm^2 length and width for feedline 2. For feedline 3, the length and width were set to 1.50×0.70 mm^2. The distance between two patches was measured as d1. When it comes to the ground, we considered the substrate. The substrate itself was measured to be 9×13 mm^2. These instructions and measurements were crucial in designing an effective and efficient array antenna.

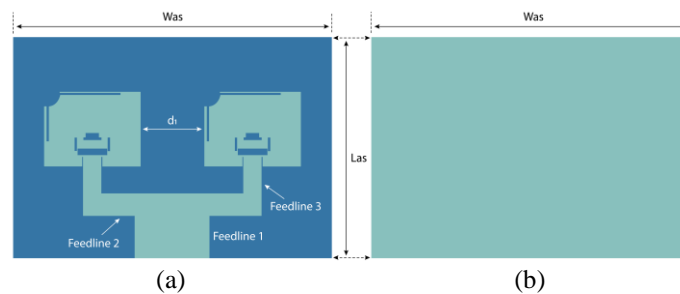(a)   (b)

Figure 2. View of proposed array antenna; (a) front and (b) back

2.3. Multiple-input multiple-output antenna

This section provides a detailed investigation of a 4-port MIMO antenna configuration and the techniques employed to grow the isolation among its components. The MIMO antenna design with dimensions of 31.75×31.75 mm^2 (Lms×Wms) is explored in depth, considering various factors such as antenna spacing, radiation patterns, and polarization. Additionally, it is positioned within a slot measuring 0.10×8 mm² on the left side of the center of a complete ground plane. The aim is to facilitate a improved understanding of the antenna's performance and characteristics. The analysis also covers the various techniques used to reduce interference and grow the signal-to-noise ratio (SNR), such as beamforming and spatial multiplexing [15]. In Figure 3, we visually represent the MIMO antenna's design where Figure 3(a) displays the front side, and Figure 3(b) shows the back side of the MIMO antenna, which is a helpful reference throughout the analysis.
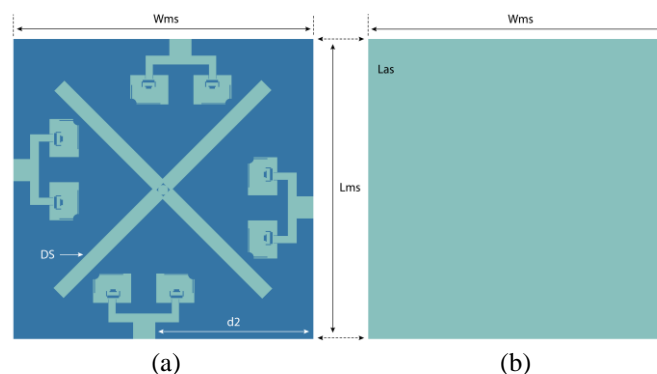

(a)   (b)

Figure 3. Design of the proposed MIMO antenna; (a) front and (b) back

3. RESULT, ANALYSIS, AND COMPARISON

Designing an antenna involves a series of steps or parameters that require adjustments to achieve an acceptable outcome. This section will delve into the outcomes of different techniques to enhance our antenna's performance and explore the impact of various parameters on the antenna's behavior.

3.1. Parametric study of single-element antenna

During the parametric study, we will explore and analyze various parameters that have impacted our antenna design process. Our goal is to gain a deeper understanding of how we can optimize these parameters to increase the performance of our antennas with parameter variation.

− Effects of modifying the width of the feed line: this section analyzes how feed line width affects antenna resonance frequency. The proposed antenna has a 0.7 mm feed line. We altered the feed line width to match the antenna resonance frequency while leaving all other parameters the same to evaluate its effect. The feed line width was investigated, ranging from 0.5 mm to 0.9 mm. Figure 4(a) shows that changing the feed line width changes the microstrip antenna's resonance frequency. Feed line width increases leftward shift and decreases resonance frequency. Conversely, lowering breadth causes a slight rightward shift and a significant resonance frequency decrease.

− Changing the slot values: slot size impacts antenna resonant frequency. The recommended antenna slot is 0.18125 mm. While keeping all other settings, the slot is tuned to the antenna's resonance frequency to analyze the slot effect. Investigations included 0.175–0.325 mm slots. Figure 4(b) indicates that slot adjustments considerably alter microstrip antenna resonance frequency. As the graph slot increases, resonance frequency falls and shifts right. However, a minor left shift and slot decrease boost resonant frequency.

− Changing the value of patch width: this section examines how the patch width affects the antenna's resonance frequency. The suggested antenna has a 3.88889 mm patch. To assess the impact of varying the patch width while keeping other parameters constant, widths ranging from 3 mm to 4.5 mm were tested. Figure 4(c) shows that increasing the patch width significantly lowers the return loss, causing a leftward resonance frequency shift. Conversely, decreasing the width notably drops the return loss, causing a minor rightward shift.
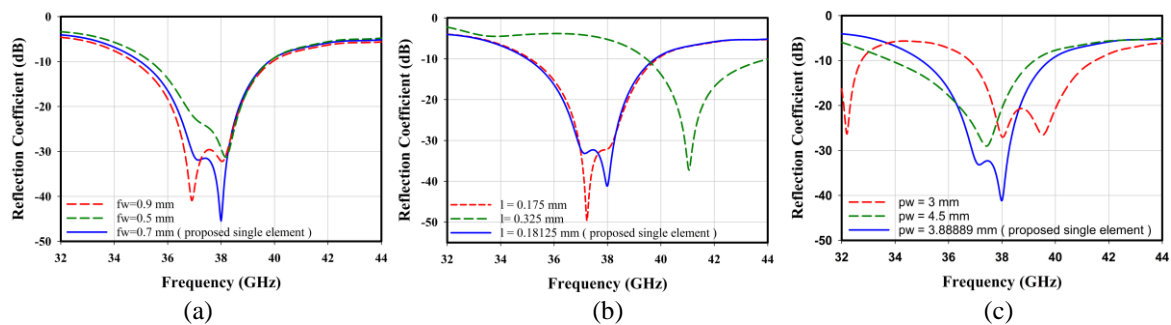

Figure 4. Single-element antenna of the reflection coefficient for different; (a) feed widths, (b) slot value, and (c) patch width

3.2. Reflection coefficient of single-element antenna

Examining the reflection coefficient of the single-element antenna in Figure 4 reveals two resonance frequencies around 38 GHz. The first exhibits a significant return loss, while the second has a low return loss. Both frequencies are encompassed by a large bandwidth, explicitly targeting the 38 GHz frequency. The measured bandwidth and reflection coefficient, at 4.808 GHz and -45.481 dB, respectively, indicate positive results. Figure 5(a) highlights the exceptional performance of our array antenna. While the single-element antenna had a bandwidth of 4.808 GHz, the array antenna's bandwidth expanded to 9.814 GHz, a significant improvement. The initial goal of developing the array antenna was to rise gain, but it also enhanced frequency range and reduced reflected energy [16]. The measurement of return loss was conducted on this array antenna. Gain in patch antennas is crucial for concentrating and directing radiated energy in specific directions [17]. Figure 5(b) shows the single-element antenna's maximum gain of 6.32 dB. The gain depends on the antenna's dimensions, configuration, direction, and signal frequency [18]. Resonance at frequencies where the single-element antenna produces more power suggests its suitability for solid signal reception and transmission. In contrast, the array antenna gains 7.71 dB, enhancing signal transmission and reception efficiency over longer distances.

Efficiency is a cornerstone of antenna design, and our single-element antenna excels with a remarkable 98% efficiency. This high efficiency is demonstrated by the antenna's performance curve, showing that most of the power is effectively radiated, enhancing signal quality and communication stability.

Figure 5(b) highlights the superior performance of our array antenna with its 99.9% efficiency. This remarkable achievement underscores the array antenna's ability to radiate most of its power, significantly improving signal quality and communication reliability [19]. Our designs provide high gain and efficiency in single-element and array antennas, making them ideal for applications requiring reliable signal transmission and reception.
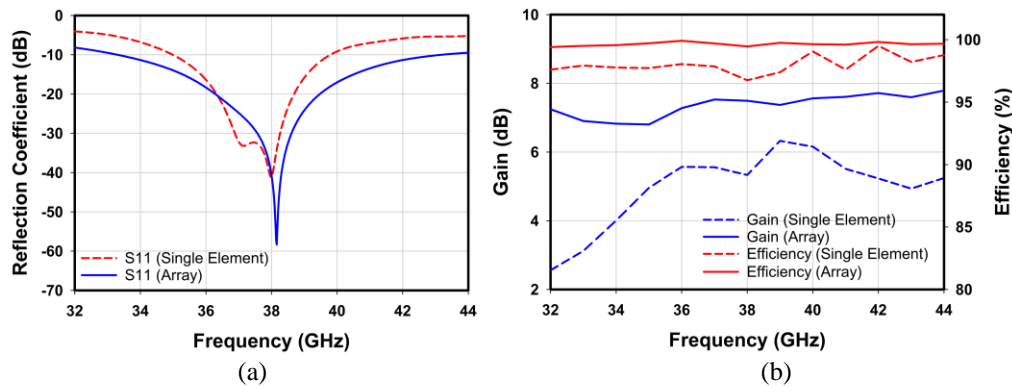

Figure 5. View single element antenna and array; (a) reflection coefficient and (b) gain and efficiency

3.2.1. Multiple-input multiple-output antenna optimization process

Figure 6(a) shows that in the first step, we attempted to design a MIMO antenna using copper for both the patch and ground. In this step, we used an array antenna as the fundamental element with a slot on the ground to create a 4-port MIMO configuration. The ground, positioned just to the left of the center, has a length of 0.10 mm and a width of 8 mm. The result shows that the resonance frequency of the microstrip antenna has changed, with the current resonance frequency being 36.68 GHz. The return loss found for this design is 26.89 dB. We kept everything the same in the second step but used x-shaped decoupling elements to improve the result. Four x-shaped pieces, each with a length of 1.50 mm and a width of 15 mm, extend from the ground slot's center to the left. This modification in the second step changes the antenna design and shifts the resonant frequency to 37.5 GHz. The return loss found for this design is 29.53 dB. In the third step, representing our proposed antenna, we fixed everything except removing the slots on the ground. This time, we achieved better results than in the previous steps, as shown in Figure 6(b). The design change resulted in a shift in the resonant frequency, with the return loss measured at -37.353 dB.
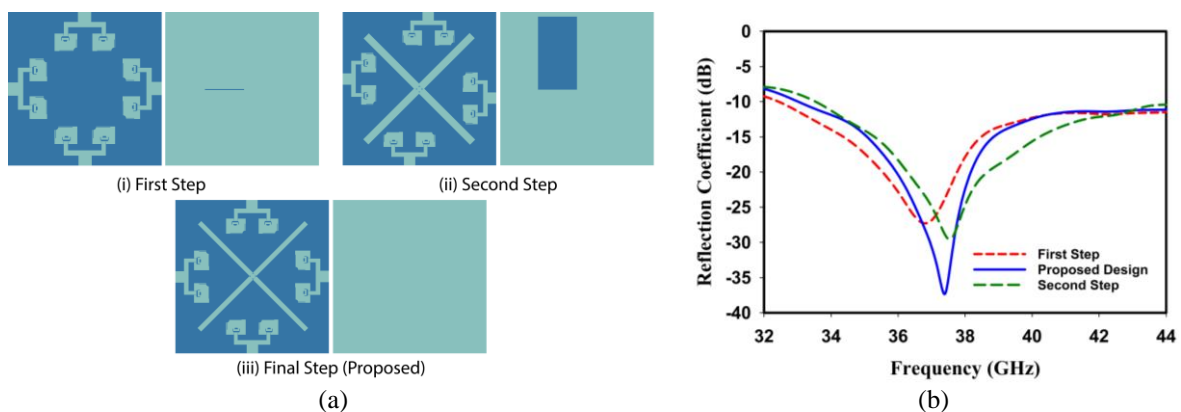

Figure 6. Proposed MIMO antenna development; (a) design steps and (b) reflection coefficient for each step

3.2.2. Proposed multiple-input multiple-output antenna's result and analysis

This segment will delve into the results of our proposed MIMO antenna. One of the primary deliberations when designing a MIMO antenna is isolation. Our MIMO antenna boasts an impressive isolation level of 28.01dB, which stands out particularly well compared to other antennas in Table 1.

Furthermore, the impressive bandwidth of our MIMO antenna is noteworthy, as achieving high bandwidth is a challenging feat. Our MIMO antenna has a bandwidth of 11.948 GHz; the return loss is measured at -37.353 dB.

Antenna design involves several important factors that affect performance. Gain and efficiency are crucial. Usually, antenna gain evaluates its capacity to focus energy [20]. Our antenna has an outstanding 8.875 dB gain, indicating exceptional precision and accuracy in signal transmission and reception. Efficiency is also essential while designing an antenna. This value represents how successfully the antenna converts input power into radiated power [21]. Our antenna's high efficiency of 98.859% reassures the audience of its performance in a reliable wireless communication system. Figure 7 illustrates the performance of the proposed MIMO antenna in terms of gain and efficiency. Figure 7(a) presents the reflection and transmission coefficients, while Figure 7(b) shows the gain and radiation efficiency.

Table 1. Performance comparison with the recent published work

Ref.	[7]	[8]	[9]	[10]	[11]	[12]	Proposed
fr	38	38	38	38	37	28/38	38
Bandwidth	1.2	3.38	2	1.4	6	1.9, 5.5	11.945
No of port	4	2	2	1	1	2	4
Dimension (mm^2)	2.53×3.04 λo	5.44×3.16 λo	3.29×1.77 λo	NA	NA	27.65×12	31.75×31.75
Gain (dB)	7.9	4.85	1.83	8.1	8.2	5.2/5.3	8.875
Efficiency (%)	85	NA	76	NA	90	NA	98.8
Isolation (dB)	28	>24	>20	NA	NA	30/22	27.627
ECC	<0.001	NA	0.001	NA	NA	<10-5	
DG	NA	NA	NA	NA	NA	9.99	9.9998
Material	Rogers RT5880	FR4	Rogers RT5880	Rogers RO3003	Rogers RT5880	Rogers RO4003	Rogers RT5880
RLC equivalent circuit	No	No	No	No	No	No	Yes
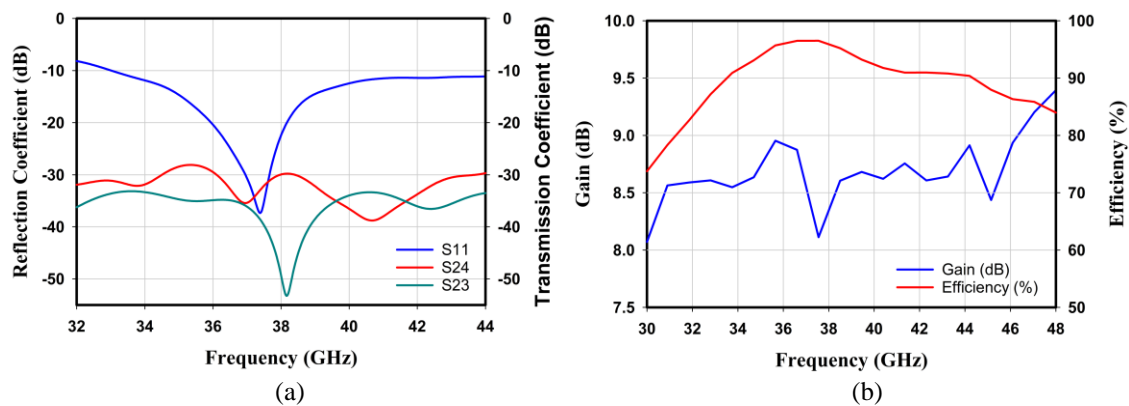
Figure 7. View of the MIMO antenna; (a) reflection and transmission coefficient and (b) gain and radiation efficiency

4. CURRENT DISTRIBUTION OF THE DESIGNED ANTENNA

Figure 8(a) shows that a single element's maximum surface current density (521.092 A/m) happens at a frequency of 38 GHz. The strongest surface current shows near the feed line and slots. By 38 GHz, Figure 8(b) shows the 1×2 array elements' peak surface current density of 159.371 A/m. The patch, connector, and feedline carry the maximum surface current in this direction. When one port is excited and the further ports are completed with matched loads, these optimization strategies help the MIMO antenna function better at 38 GHz. Except for antenna 1, which is activated by a surface current, the antennas do not exhibit a significant amount of surface current, as seen in Figures 8(c) and 8(d). Turning on just antenna 2 prevents the other antennas from producing surface currents. When antenna 3 or antenna 4 is aroused, the same happens in Figures 8(e) and 8(f).
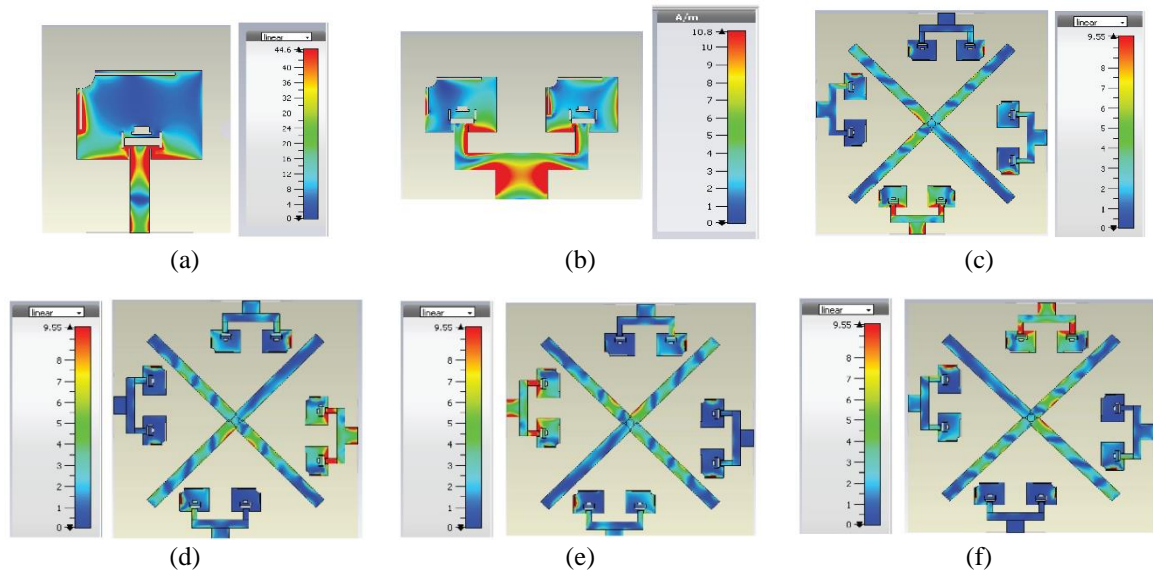
Figure 8. Current distribution of; (a) single-element, (b) array antenna, (c) MIMO (Ant. 1), (d) MIMO (Ant. 2), (e) MIMO (Ant. 3), and (f) MIMO (Ant. 4)

5. RADIATION PATTERN

A radiation pattern directly describes an antenna's power in space. Two main electromagnetic field components surround an antenna: the electric field (E-field) and the magnetic field (H-field). Figure 9 illustrates the XZ cut at $\Phi=0°$, also referred to as the E-plane of the radiation pattern. On the other hand, the configuration in question, which remains at a fixed angle of 90° and varies between 0° and 360° [22], is denoted as the YZ cut ($\Phi=90°$) in Figure 9 and is also known as the H-plane. The lobe's initial focus, which corresponds to 44 GHz, is positioned at (3460, 16.40) for (0°, 90°). At angles of 0° and 90°, the amplitude of the initial lobe of the E-field is 18.8- and 16.4-dB V/m, respectively. The H-field has a half-power beam width (HPBW) of 38.7°, an initial lobe magnitude of -32.4 dB A/m at phi=9°, whereas the 3 dB angular beam width at $\varphi=90°$ is 14.50 at 44 GHz.
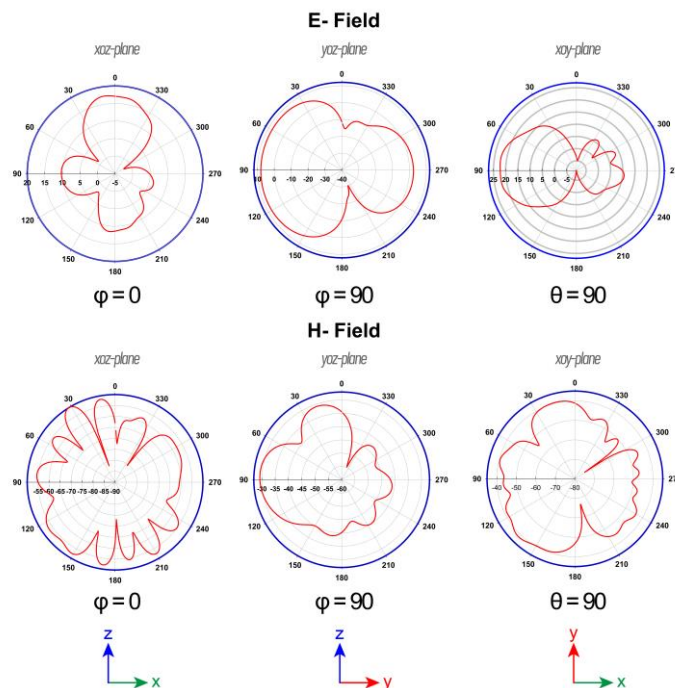
Figure 9. View proposed MIMO antenna normalized radiation pattern

6.   ENVELOP CORRELATION COEFFICIENT AND DIVERSITY GAIN

To evaluate the functionality of the MIMO antenna method, it is essential to analyze exact attributes usually known as "MIMO performance metrics." These metrics can be calculated after the S-Parameters, providing worthy information on how common coupling and antenna impedance similarly touch the diversity presentation of the MIMO antenna. The ECC, a measure used to gauge the similarity of radiation patterns from changed antennas, is not just a theoretical concept. It has real-world implications. A calculated value of ECC less than 0.0008 was determined, indicating the practicality of the MIMO antenna. In an uncorrelated MIMO antenna, the ideal ECC value is zero, but in practical MIMO situations, maintaining ECC below or equal to 0.5 across the entire usable frequency range is advisable [23]. Figure 10 visually represents the antenna's envelope correlation coefficient, reinforcing the practicality of our work.

$$ECC = \frac{\left|s_{ii}^* s_{ij} + s_{ji}^* s_{jj}\right|^2}{\left(\left(1 - |s_{ii}|^2 - |s_{ij}|^2\right)\left(1 - |s_{ji}|^2 - |s_{jj}|^2\right)\right)}$$

To improve the reliability of the radio connection, we measured the diversity gain for a set of antennas with ECC=0 and found it to be 10 dB [24]. However, the performance of the MIMO system is contrarily impacted by the correlation among its antenna components, resulting in $\sqrt{1 - ECC^2}$. As such, we can determine the diversity gain. Of the MIMO system with connected antenna essentials using the provided equation, Figure 10 shows the antenna's diversity gain, which is a favorable value of 9.9998 dB.

$$DG = 10\sqrt{1 - ECC^2}$$
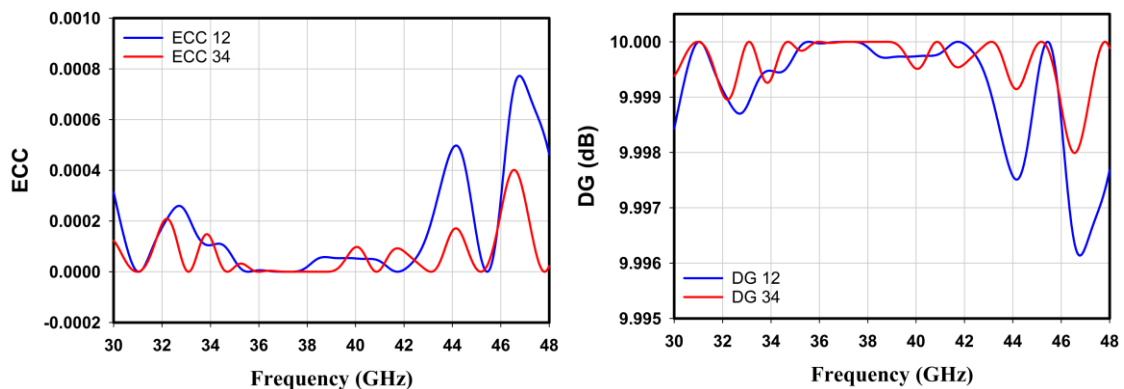
Figure 10. ECC and DG of proposed MIMO antenna

7.   RESISTOR, INDUCTOR, AND CAPACITOR EQUIVALENT CIRCUIT

Figure 11 shows the circuit diagram of the MIMO antenna. The impedance investigation function in CST Studio, a simulation and circuit pattern software, can be used to assess the values of RLC [25]. Agilent ADS is a component of the environment. The parameter names of components L1, C1, and R1 establish the frequency. A series circuit of L8, C8, and R3 represents the main feed line, and C3, L3, and C4, L4 represents the branching feedline of the array antenna. Finally, the circuit of the four-array antenna is combined to make the circuit of the proposed MIMO antenna. The capacitance and inductance among antenna 1 and antenna 2 are determined by the components L10 and C10, correspondingly. Similarly, the same parameters for antennae 2 and 3 are determined by C13 and L13. The inductance and capacitance among antenna 3 and 4 are dictated by the values of C12 and L12, respectively. Similarly, the values of C14 and L14 define the inductance and capacitance among antenna 1 and antenna 4. Antenna 2 and antenna 4 share elements C11 and L11. The values of capacitance and inductance among antenna 1 and antenna 3 are determined by the components C9 and L9. The values of the circuit components are provided in the table. This model can be used to evaluation the performance of the proposed MIMO antenna. Figure 12 shows the result of the simulation conducted using CST and the equivalent RLC circuit result obtained from ADS.
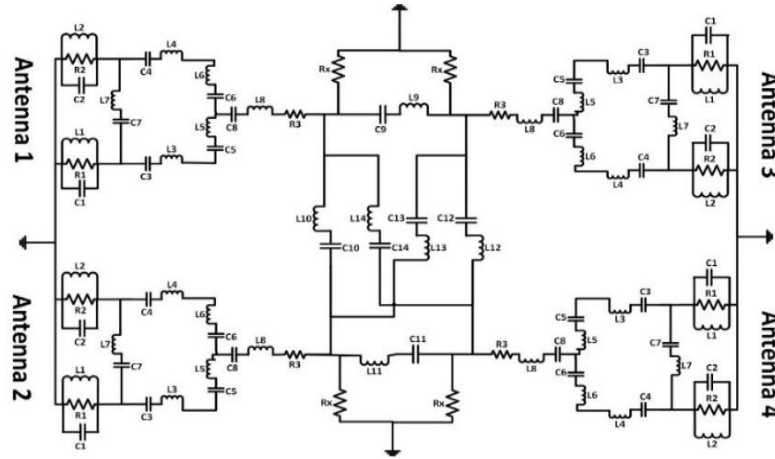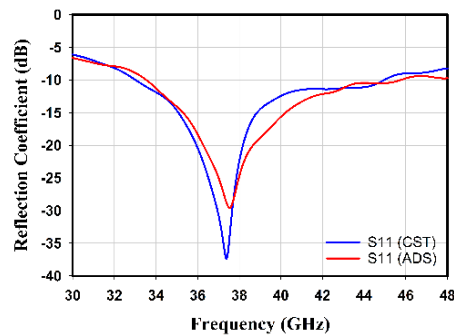
Figure 11. RLC of the proposed antenna

Figure 12. Simulated equivalent circuit reflection coefficient in ADS and CST

8. CONCLUSION

Its comprehensive development of CST simulation tools demonstrates the design's exceptional accuracy. Each element has dimensions of 7×7 mm² and a bandwidth of 4.81 GHz. The system's efficiency is 97.81%, which indicates its remarkable performance. Additionally, the gain is measured at 7.604 dB. In the 1x2 array configuration, the bandwidth significantly rose from 4.81 GHz to 9.814 GHz, while efficiency improved significantly from 97.81% to 99.74%. The MIMO design resulted in the antenna achieving ideal performance, exhibiting a gain of roughly 8.875 dB and a bandwidth of 11.952 GHz. By designing and simulating a similar RLC circuit in ADS, we have verified the precision and dependability of the data obtained via CST. The CST and ADS simulators produced comparable reflection coefficients.

REFERENCES

[1] A. Abhishek and P. Suraj, "A Compact Patch Antenna for 5G Communication (39 GHz-mmWave-n260) Employing Aperture Coupled Feeding Technique," *Wireless Personal Communications*, vol. 135, no. 2, pp. 1259–1284, Mar. 2024, doi: 10.1007/s11277-024-11127-x.
[2] A. Hazarika and M. Rahmati, "Towards an Evolved Immersive Experience: Exploring 5G- and Beyond-Enabled Ultra-Low-Latency Communications for Augmented and Virtual Reality," *Sensors*, vol. 23, no. 7, p. 3682, Apr. 2023, doi: 10.3390/s23073682.
[3] A. K. Arya, S. J. Kim, and S. Kim, "A Dual-Band Antenna for Lte-R and 5G Lower Frequency Operations," *PIER Letters*, vol. 88, pp. 113–119, 2020, doi: 10.2528/PIERL19081502.
[4] P. Tiwari, V. Gahlaut, M. Kaushik, P. Rani, A. Shastri, and B. Singh, "Advancing 5G Connectivity: A Comprehensive Review of MIMO Antennas for 5G Applications," *International Journal of Antennas and Propagation*, vol. 2023, pp. 1–19, Aug. 2023, doi: 10.1155/2023/5906721.

[5]   O. O. Erunkulu, A. M. Zungeru, C. K. Lebekwe, M. Mosalaosi, and J. M. Chuma, "5G Mobile Communication Applications: A Survey and Comparison of Use Cases," *IEEE Access*, vol. 9, pp. 97251–97295, 2021, doi: 10.1109/ACCESS.2021.3093213.

[6]   A. A. El-Saleh *et al.*, "Measuring and Assessing Performance of Mobile Broadband Networks and Future 5G Trends," *Sustainability*, vol. 14, no. 2, p. 829, Jan. 2022, doi: 10.3390/su14020829.

[7]   K. Raheel *et al.*, "E-Shaped H-Slotted Dual Band mmWave Antenna for 5G Technology," *Electronics*, vol. 10, no. 9, p. 1019, Apr. 2021, doi: 10.3390/electronics10091019.

[8]   F. F. Kiouach, M. El Ghzaoui, S. Varakumari, R. El Alami, and S. Das, "A Low-profile Wideband Two Ports MIMO Antenna Working at 38 GHz for mm-wave 5G Applications," *Journal of Nano- and Electronic Physics*, vol. 15, no. 1, pp. 01025-1-01025–5, 2023, doi: 10.21272/jnep.15(1).01025.

[9]   M. N. Hasan, S. Bashir, and S. Chu, "Dual band omnidirectional millimeter wave antenna for 5G communications," *Journal of Electromagnetic Waves and Applications*, vol. 33, no. 12, pp. 1581–1590, Aug. 2019, doi: 10.1080/09205071.2019.1617790.

[10]   S. N. Nafea and N. N. Khamiss, "For 5G applications, high-gain patch antenna in Ka-Band," *Indonesian Journal of Electrical Engineering and Computer Science*, vol. 31, no. 2, pp. 802-809, Aug. 2023, doi: 10.11591/ijeecs.v31.i2.pp802-809.

[11]   S. M. Shamim, U. S. Dina, N. Arafin, and S. Sultana, "Design of Efficient 37 GHz Millimeter Wave Microstrip Patch Antenna for 5G Mobile Application," *Plasmonics*, vol. 16, no. 4, pp. 1417–1425, Aug. 2021, doi: 10.1007/s11468-021-01412-x.

[12]   A. R. Sabek, W. A. E. Ali, and A. A. Ibrahim, "Minimally Coupled Two-Element MIMO Antenna with Dual Band (28/38 GHz) for 5G Wireless Communications," *Journal of Infrared, Millimeter, and Terahertz Waves*, vol. 43, no. 3–4, pp. 335–348, Mar. 2022, doi: 10.1007/s10762-022-00857-3.

[13]   Md. A. Haque *et al.*, "Machine learning-based technique for gain prediction of mm-wave miniaturized 5G MIMO slotted antenna array with high isolation characteristics," *scientific reports*, vol. 15, no. 1, p. 276, Jan. 2025, doi: 10.1038/s41598-024-84182-w.

[14]   D. Bu, S. -W. Qu and S. Yang, "Planar, Ultra-Wideband and Dual-Polarized Phased Array Antenna for Millimeter-Wave Vehicular Communication," *IEEE Transactions on Vehicular Technology*, vol. 73, no. 7, pp. 9972-9983, Jul. 2024, doi: 10.1109/TVT.2024.3364251.

[15]   P. Tiwari, V. Gahlaut, U. N. Mishra, A. Shastri, and M. Kaushik, "Polarization diversity configuration of millimeter wave MIMO antenna for Ka-band application in 5G wireless networks," *Journal of Electromagnetic Waves and Applications*, vol. 38, no. 4, pp. 486–507, Mar. 2024, doi: 10.1080/09205071.2024.2319683.

[16]   C.-Y.-D. Sim, J.-J. Lo, and Z. N. Chen, "Design of a Broadband Millimeter-Wave Array Antenna for 5G Applications," *IEEE Antennas and Wireless Propagation Letters*, vol. 22, no. 5, pp. 1030–1034, May 2023, doi: 10.1109/LAWP.2022.3231358.

[17]   K. Cuneray, N. Akcam, T. Okan, and G. O. Arican, "28/38 GHz dual-band MIMO antenna with wideband and high gain properties for 5G applications," *AEU - International Journal of Electronics and Communications*, vol. 162, p. 154553, Apr. 2023, doi: 10.1016/j.aeue.2023.154553.

[18]   I. U. Din *et al.*, "Improvement in the Gain of UWB Antenna for GPR Applications by Using Frequency-Selective Surface," *International Journal of Antennas and Propagation*, vol. 2022, pp. 1–12, Oct. 2022, doi: 10.1155/2022/2002552.

[19]   Md. K. Ahmed *et al.*, "ANN-based performance estimation of a slotted inverted F-shaped tri-band antenna for satellite/mm-wave 5G application," *TELKOMNIKA (Telecommunication Computing Electronics and Control)*, vol. 22, no. 4, pp. 773-783, Aug. 2024, doi: 10.12928/telkomnika.v22i4.26028.

[20]   S. Maity, T. Tewary, S. Mukherjee, A. Roy, P. P. Sarkar, and S. Bhunia, "Super wideband high gain hybrid microstrip patch antenna," *AEU - International Journal of Electronics and Communications*, vol. 153, p. 154264, Aug. 2022, doi: 10.1016/j.aeue.2022.154264.

[21]   M. A. Haque *et al.*, "A Modified E-Shaped Microstrip Patch Antenna for C Band Satellite Applications," in *2019 IEEE International Conference on Signal Processing, Information, Communication & Systems (SPICSCON)*, Dhaka, Bangladesh: IEEE, Nov. 2019, pp. 27–31, doi: 10.1109/SPICSCON48833.2019.9065126.

[22]   L. C. Paul *et al.*, "Design a slotted metamaterial microstrip patch antenna by creating three dual isosceles triangular slots on the patch and bandwidth enhancement," in *2017 3rd International Conference on Electrical Information and Communication Technology (EICT)*, Khulna: IEEE, Dec. 2017, pp. 1–6, doi: 10.1109/EICT.2017.8275143.

[23]   A. K. Singh and S. Pal, "Compact Self-Isolated Extremely Low ECC Folded-SIW-Based Slot MIMO Antenna for 5G Application," *IEEE Antennas and Wireless Propagation Letters*, vol. 23, no. 1, pp. 194-198, Jan. 2024, doi: 10.1109/LAWP.2023.3321065.

[24]   S. Xi, J. Cai, L. Shen, Q. Li, and G. Liu, "Dual-Band MIMO Antenna with Enhanced Isolation for 5G NR Application," *Micromachines*, vol. 14, no. 1, p. 95, Dec. 2022, doi: 10.3390/mi14010095.

[25]   Md. A. Haque *et al.*, "Dual Band Antenna Design and Prediction of Resonance Frequency Using Machine Learning Approaches," *Applied Sciences*, vol. 12, no. 20, p. 10505, Oct. 2022, doi: 10.3390/app122010505.

BIOGRAPHIES OF AUTHORS

Md. Ashraful Haque 🆔 ⑧ⁱ SC ◗ is doing Ph.D. at the Department of Electrical and Electronic Engineering, Universiti Teknologi PETRONAS, Malaysia, He got his B.Sc. in electronics and electronic engineering (EEE) from Bangladesh's Rajshahi University of Engineering and Technology (RUET) and his M.Sc. in the same field from Bangladesh's Islamic University of Technology (IUT). He is currently on leave from Daffodil International University (DIU) in Bangladesh. His research interest includes microstrip patch antenna, sub 6 5G application, and supervised regression model machine learning on antenna design. He can be contacted at email: limon.ashraf@gmail.com.

Md. Kawsar Ahmed is currently pursuing his studies in the field of electrical and electronic engineering at Daffodil International University. He successfully finished his Higher Secondary education at Agricultural University College, Mymensingh. He is presently employed as an Assistant Administrative Officer at the Office of Students' Affairs at Daffodil International University (DIU) in Bangladesh. The areas of his research focus encompassed microstrip patch antennas, terahertz antennas, and applications related to 4G and 5G technologies. He can be contacted at email: kawsar33-1241@diu.edu.bd.

Narinderjit Singh Sawaran Singh is an Associate Professor in INTI International University, Malaysia. He graduated from the Universiti Teknologi PETRONAS (UTP) in 2016 with Ph.D. in electrical and electronic engineering specialized in probabilistic methods for fault tolerant computing. Currently, he is appointed as the research cluster head for computational mathematics, technology, and optimization which focuses on the areas like pattern recognition and symbolic computations, game theory, mathematical artificial intelligence, parallel computing, expert systems and artificial intelligence, quality software, information technology, exploratory data analysis, optimization algorithms, stochastic methods, data modelling, and computational intelligence-swarm intelligence. He can be contacted at email: narinderjits.sawaran@newinti.edu.my.

Md. Afzalur Rahman is working as an Assistant Engineer in a consultancy firm named Fire and Electrical Solutions, Dhaka, Bangladesh. He is from Cumilla, Bangladesh. He has completed his B.Sc. in engineering degree in electrical and electronics engineering (EEE) from Daffodil International University in 2022. Before that, he completed his Higher Secondary School Certificate from Bangladesh Navy College, Dhaka, Bangladesh, and his Secondary School Certificate from Cumilla Modern High School, Cumilla, Bangladesh. He can be contacted at email: afzalur33-4556@diu.edu.bd.

Md. Sharif Ahammed is a student of Daffodil International University and pursuing a B.Sc. in the Department of Electrical and Electronics. He passed from Government Bangabandhu college with a higher secondary. Microstrip patch antenna, terahertz antenna, and 5G application are some of his research interests. He can be contacted at email: sharif33-1152@diu.edu.bd.

Redwan A. Ananta is currently studying B.Sc. in Department of Electrical and Electronics at Daffodil International University. He passed higher secondary from Adamjee Cantonment College. His research focuses on advanced antenna technologies for mm-wave, 5G, 6G, sub-6 GHz, and THz frequencies. He can be contacted at email: redwan33-1145@diu.edu.bd.

Kamal Hossain Nahin [iD] [g] [SC] [C] currently pursuing a degree in electrical and electronic engineering at Daffodil International University. His educational journey began at Ishwardi Govt College for his Higher Secondary Certificate (HSC). As a budding researcher in the communication field, he is passionate about wireless communication, focusing on microstrip patch antennas, terahertz antennas, and their potential applications in future 5G and 6G technologies. He can be contacted at email: kamal33-1242@diu.edu.bd.

Jamal Hossain Nirob [iD] [g] [SC] [C] is a student in the Department of Electrical and Electronic Engineering (EEE) at Daffodil International University. His educational journey began at Maniknagar High School, where he successfully completed his Secondary School Certificate (SSC). Following that, he pursued higher studies at Ishwardi Government College, obtaining his Higher Secondary Certificate (HSC). With a strong enthusiasm for expanding communication technology, Jamal has focused his research on wireless communication, specifically on microstrip patch antennas, terahertz antennas, and applications of 5G and 6G. He can be contacted at email: jamal33-1243@diu.edu.bd.

Liton Chandra Paul [iD] [g] [SC] [C] successfully completed his master's in electrical and electronic engineering (EEE) in 2012 and his bachelor's in electronics and telecommunication engineering (ETE) in 2015. As a student, he actively contributed to various nonprofit organizations. He currently serves as an advisor for IEEE PUST SB and IEEE PUST AP-S SB Chapter, and as a student activity coordinator for IEEE APS-MTTS BD Joint Chapter. He is also an ambassador for IEEE Day 2024. His research interests include RFIC, bioelectromagnetics, microwave technology, antennas, phased arrays, and mmWave. He can be contacted at: litonpaulete@gmail.com.